Journal of Electrochemistry

Volume 23 | Issue 4

2017-08-25

An investigation of the synergistic effect between (1,3-Dioxolan-2-ylmethyl)triphenylphosphonium bromide and iodide ion for the corrosion inhibition of zinc in citric acid

Saadawy M.
Chemistry Department, Faculty of Science, Alexandria University, Egypt Ibrahimia, El-Horeya Street P.O. BOX 426 Alexandria 21321;, marwan.saadawy@yahoo.com

Recommended Citation
Saadawy M.. An investigation of the synergistic effect between (1,3-Dioxolan-2-ylmethyl)triphenylphosphonium bromide and iodide ion for the corrosion inhibition of zinc in citric acid[J]. *Journal of Electrochemistry*, 2017 , 23(4): 441-455.
DOI: 10.13208/j.electrochem.151222
Available at: https://jelectrochem.xmu.edu.cn/journal/vol23/iss4/9

This Article is brought to you for free and open access by Journal of Electrochemistry. It has been accepted for inclusion in Journal of Electrochemistry by an authorized editor of Journal of Electrochemistry.

DOI: 10.13208/j.electrochem.151222 **Artical ID**:1006-3471(2017)04-0441-15
Cite this: *J. Electrochem.* **2017**, *23*(4): 441-455 **Http**://electrochem.xmu.edu.cn

An Investigation of the Synergistic Effect between (1,3-Dioxolan-2-ylmethyl)-Triphenylphosphonium Bromide and Iodide Ion for the Corrosion Inhibition of Zinc in Citric Acid

M. Saadawy*
(*Chemistry Department, Faculty of Science, Alexandria University, Egypt Ibrahimia, El–Horeya Street P.O. BOX* 426 *Alexandria* 21321)

Abstract: The effect of (1,3-Dioxolan-2-ylmethyl)-triphenylphosphonium bromide (DTPB) on the zinc corrosion in 0.5 mol·L^{-1} citric acid solution was investigated at 30 ºC using weight loss, potentiodynamic polarization and electrochemical impedance spectroscopy (EIS) techniques. An ecofriendly bath was used for acid cleaning of zinc, which has not been widely used in literatures. The results showed that DTPB could serve as an effective inhibitor for the zinc corrosion in a citric acid solution with the inhibition efficiency of 98.9% at the DTPB concentration of 3×10^{-3} mol·L^{-1}. A synergistic effect between DTPB and potassium iodide (KI) enhanced the inhibition capability of DTPB, and better inhibition efficiency was achieved as compared with that by using DTPB alone. The synergism parameter had a value of 1.2 and was found to decrease with temperature. An inhibition mechanism is proposed by which KI acts as an adsorption mediator for bonding metal surface and DTPB.

Key words: zinc; polarization; electrochemical impedance spectroscopy; acid corrosion; synergism
CLC Number: O646 **Document Code**: A

Zinc has gained a great attention due to its great deal of practical application and use; it is utilized as a reactive anode in electrochemical energy generators, in galvanization and in the case of atmospheric corrosion. Moreover zinc and its alloys are extensively utilized in the forms of castings, forgings, rolled sheets, extrusions and coatings in various industrial and technological applications[1]. Zinc oxide is used in rubber tires, white paint pigment, ceramic glaze, opaque bases in cosmetics and in catalysis. Therefore, the zinc corrosion and inhibition are a subject of practical significance[2-9]. The corrosion resistance of zinc depends on its ability to form a protective layer by reacting with its surrounding environment, nevertheless, zinc metal is highly susceptible to corrosion by acids. It is, therefore, necessary to utilize inhibitors for scale removal and cleaning of zinc surfaces with acidic solutions[10]. Most of these inhibitors would decrease the corrosion rate by increasing the hydrogen over potential on the corroding metal[11] and would be adsorbed on the metal surface to block the active sites. Numerous organic compounds have been previously investigated as inhibitors for the corrosion of zinc in different leaching mineral acids such as hydrochloric acid (HCl)[12-13], sulfuric acid (H_2SO_4)[14-15], nitric acid (HNO_3)[16], phosphoric acid[17-18] and perchloric acid[19]. Among these mineral acids, H_2SO_4 has been reported as the most preferred lixiviant[20]. The known hazardous effects of most synthetic corrosion inhibitors motivated the alternative use of some natural products as safe corrosion inhibitors as they are rich in compounds containing electron-donating groups like oxygen, sulphur and nitrogen, therefore, can be widely utilized as corrosion inhibitors of zinc metal in acidic media[21-22]. This revolution concerning the uses of natural products or plant extracts as corrosion inhibitors for metals in acid baths of mineral acids had three disadvantages. First, the inhibition

Received: 2015-12-22, Revised: 2016-04-14 *Corresponding author, Tel: (002-012)24570665, E-mail: marwan.saadawy@yahoo.com

mechanism cannot be completely understood by these green compounds containing numerous extracted species due to the difficulty in recognizing the exact adsorbed effective compounds among hundreds of compounds present in the plant extract. Second, mineral acids usually cause environmental pollution and may release undesired impurities by dissolving. Third, mineral acids used in acid cleaning bath are usually present in a large amount. Therefore, it is more worthy using an environmentally friendly acid bath than using a green inhibitor which is usually present in a trace amount.

Organic acids have low dissolution efficiency at mildly acidic conditions (pH 3 ~ 5) and can be easily extracted by simple procedures with low cost from vegetables or fruits. A synergistic inhibition effect, which is a combined action of compounds greater in total effect than the sum of individual effects, can be well-achieved by introducing smallest amounts of synthetic inhibitor which is usually organic compound containing different functional groups with another ionic species that enhances the inhibition capability of the inhibitor causing its small concentration to have a great percentage of inhibition[23-31]. Citric acid is best chosen among organic acids since it is available in most cheap fruits; moreover, it was used in electroplating baths of metals[32]. There has only been a small amount of research[33-38] that has dealt with the corrosion of different metals in citric acid. Literature lacks the best trial of synergistic inhibition in the safe and naturally occurring citric acid cleaning bath which can be best used for acid cleaning of zinc since it was used as an alternative lixiviant for zinc oxide dissolution[39] and it was found that a low concentration (0.05 mol·L^{-1}) of citric acid was able to dissolve 90.4% of ZnO after 1 h at 50 ℃. Therefore, the aim of the present research is to test the inhibitive action of (1, 3-dioxolan-2-ylmethyl)-riphenylphosphonium bromide (DTPB) that boasts the advantage of possessing more than one central hetero atom and multi ring system on the acidic corrosion of zinc in a safe and cheap bath of citric acid. Possible synergistic effect of iodide ion on inhibition mechanism at different temperatures is discussed in order to obtain an environmentally-friendly acid cleaning bath with best metal protection using minimum concentration of the inhibitor.

1 Experimental

1.1 Electrochemical Tests

Electrochemical impedance spectroscopic (EIS) and polarization measurements were carried out using a frequency response analyzer Gill AC instrument. The frequency range for EIS measurements was 0.1 ~ 1000 Hz with an applied potential signal amplitude of 10 mV around the rest potential. Polarization measurements were carried out at a scan rate of 0.2 mV·s^{-1} utilizing a three-electrode cell. A platinum sheet and saturated calomel electrode (SCE) were used as the counter and reference electrodes, respectively. The reference electrode was maintained in contact with electrolyte by insertion through the Luggin capillary. The luggin capillary tip was placed at 1 ~ 5 mm from the electrode surface to minimize liquid-junction or thermal junction potential. The working electrode was constructed with the zinc specimen having the following compositions (mass percentage): 0.00001 As, 0.001 P, 0.01 Pb, 0.005 Fe and balance Zn.

These zinc samples were fixed in poly tetrafluoro ethylene (PTFE) rods by an epoxy resin in such a manner that only one surface was left uncovered. The exposed area (1 cm^2) was mechanically polished with a series of emery papers of variable grades, starting with a coarse one and proceeding in steps to the finest grade 1200. The samples were then washed thoroughly with double distilled water followed with A.R. ethanol, and finally with distilled water just before insertion into the cell.

1.2 Weight-Loss Measurement

The experiments were executed utilizing rectangular zinc coupons, each with an area of 6 cm^2 and with the same chemical composition of the zinc samples utilized in the electrochemical measurements. The weighed coupons, after polishing and cleaning, were suspended in beakers containing the test solution. After different days of exposure, the coupons

were removed from the solution, washed with distilled water, dried with ethanol followed by acetone and then reweighed. The weight loss was then determined and the rate of corrosion was expressed in $g \cdot cm^{-2} \cdot h^{-1}$. To test the reliability and reproducibility of the measurements, the experiments were repeated three times in each case at the same conditions and their mean value was recorded.

1.3 Optical Microscopic Examination

Optical micrographs (40×) were taken with a Euromex optical microscope with color video camera that is connected to a personal computer.

1.4 Solution Preparation

(1,3-dioxolan-2-ylmethyl)-triphenylphosphonium bromide (DTPB), Fig. 1, was purchased from Aldrich Chemicals Company with 98% purity.

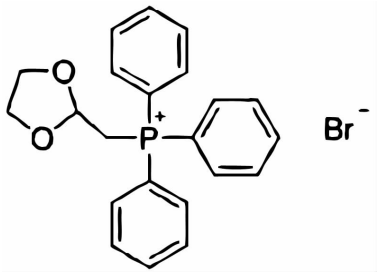

Fig. 1 (1, 3-dioxolan-2-ylmethyl)-triphenylphosphonium bromide (DTPB)

The synthesis steps of DTPB were present[40] in details and many of its physical and related properties are listed[41]. It is stable compound that undergoes decomposition into different decomposition products only by exposure to fire. The solutions were prepared utilizing double distilled water. Stock solutions of 2 $mol \cdot L^{-1}$ citric acid, 0.01 $mol \cdot L^{-1}$ DTPB and 0.1 $mol \cdot L^{-1}$ KI solutions were utilized to prepare solutions containing 0.5 $mol \cdot L^{-1}$ citric acid and the desired DTPB or KI concentrations utilizing appropriate dilutions. The concentration of the stock solution was expressed in term of moles per litre. The solution of 0.5 $mol \cdot L^{-1}$ citric acid + 10^{-3} $mol \cdot L^{-1}$ KI was prepared by mixing 25 mL of 2 $mol \cdot L^{-1}$ citric acid and 1 mL of 0.1 $mol \cdot L^{-1}$ KI then completing it to 100 mL distilled water in the cell. The solution of 0.5 $mol \cdot L^{-1}$ citric acid + 10^{-5} $mol \cdot L^{-1}$ DTPB + 10^{-3} $mol \cdot L^{-1}$ KI was prepared by mixing 25 mL of 2 $mol \cdot L^{-1}$ citric acid, 0.1 mL of 0.01 $mol \cdot L^{-1}$ DTPB and 1 mL of 0.1 $mol \cdot L^{-1}$ KI then completing it to 100 mL distilled water in the cell.

1.5 Spectrophotometric UV Analysis

For UV-visible measurements, solutions of 0.5 $mol \cdot L^{-1}$ citric acid containing 10^{-3} $mol \cdot L^{-1}$ Zn^{2+} ions, 0.5 $mol \cdot L^{-1}$ citric acid containing 10^{-3} $mol \cdot L^{-1}$ Zn^{2+} ions with 10^{-4} $mol \cdot L^{-1}$ DTPB, 0.5 $mol \cdot L^{-1}$ citric acid containing 10^{-3} $mol \cdot L^{-1}$ Zn^{2+} ions with 10^{-3} $mol \cdot L^{-1}$ KI and 0.5 $mol \cdot L^{-1}$ citric acid containing 10^{-3} $mol \cdot L^{-1}$ Zn^{2+} ions with both 10^{-4} $mol \cdot L^{-1}$ DTPB and 10^{-3} $mol \cdot L^{-1}$ KI were used. The UV-visible spectrum was achieved by using a Jasco V-530 spectrophotometer.

2 Results and Discussion

2.1 Inhibition Efficiency Analysis

Fig. 2 illustrates the variation of the inhibition efficiency, *IE*(%), with the logarithmic concentration of DTPB in 0.5 $mol \cdot L^{-1}$ citric acid after different exposure time at 30 ℃.

The values of *IE* (%) are calculated utilizing the relation:

$$IE(\%) = \frac{w_0 - w}{w_0} \times 100 \quad (1)$$

where w_0 and w are the rates of corrosion ($g \cdot cm^{-2} \cdot h^{-1}$) in the absence and presence of DTPB, respectively. The data in Fig. 2 indicates that the inhibition efficiency increased with increasing the DTPB concentration. A

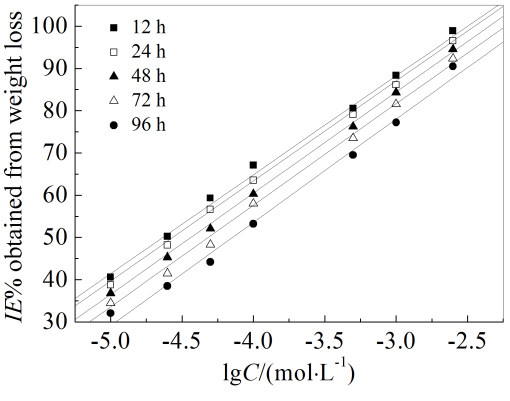

Fig. 2 Variation of the inhibition efficiency with the logarithmic concentration of DTPB in 0.5 $mol \cdot L^{-1}$ citric acid after different exposure time at 30 ℃

considerable value of 98.9% of inhibition was obtained at a concentration of 3×10^{-3} mol·L^{-1} DTPB after 12 h, which decreased only to 97.5% after 96 h exposure, indicating that the DTPB could serve as an efficient corrosion inhibitor for zinc in the citric acid solution and confirming its function persistency with time. The smallest concentrations of DTPB, 10^{-5} mol·L^{-1} and also 10^{-4} mol·L^{-1}, were chosen to test the effect on the corrosion of the metal when combined with KI. The corrosion behaviors of zinc in 0.5 mol·L^{-1} citric acid free from and containing 10^{-5} or 10^{-4} mol·L^{-1} DTPB were examined in the absence and presence of 10^{-3} mol·L^{-1} KI at 30 ℃. The values of *IE*(%) are presented in Tab. 1. It is evident that the inhibition efficiency increased markedly by the addition of both DTPB and KI more than the addition of any of DTPB or KI alone, indicating that KI greatly promotes the anti-corrosion capability of DTPB and that a combination of DTPB and KI can be utilized as good corrosion inhibitor for zinc in the citric acid solution.

2.2 Visual Inspection

Fig. 3 demonstrates photographs of zinc panels submerged for 3 h in 0.5 mol·L^{-1} citric acid free from and containing 10^{-4} mol·L^{-1} DTPB in the absence and presence of 10^{-3} mol·L^{-1} KI. It is clear that the zinc surface in the inhibitor-free solution showed severe uniform corrosion, while for the acid solution containing any of DTPB or KI, the corrosion was less severe than for the pure acid, but DTPB provided better protection than KI. On the other hand, in the presence of both DTPB and KI, there was a very mild corrosion and the scratch mark of the emery paper was still viewed after the experimental exposure time; this confirms the supporting effect of KI for DTPB as a corrosion inhibitor for zinc in citric acid solution.

2.3 Optical Micrograph

The optical microscopic photos (40 ×) for zinc submerged for 24 h in 0.5 mol·L^{-1} citric acid free from and containing 10^{-5} mol·L^{-1} DTPB in the absence and presence of 10^{-3} mol·L^{-1} KI are viewed in Fig. 4. The zinc surface in the inhibitor-free solution showed severe uniform corrosion with blocks of corrosion products, while for the acid solution containing any of DTPB or KI, the corrosion was less severe than for the pure acid. On the other hand, in the presence of both DTPB and KI, the scratch mark of the emery paper was still observed after the experimental exposure time, confirming the supporting effect of KI for DTPB as a corrosion inhibitor for zinc in citric acid solution.

2.4 Potentiodynamic Polarization Results

Typical potentiodynamic polarization curves for zinc in 0.5 mol·L^{-1} citric acid in the absence and presence of different DTPB concentrations at 30 ℃ are illustrated in Fig. 5. It is clear that the addition of DTPB affected both anodic and cathodic parts of the polarization curves, this indicates that it could be classified as a mixed-type inhibitor.

The corrosion current density was calculated from the intersection of cathodic and anodic Tafel lines, and the values of the electrochemical parameters including corrosion potential (E_{corr}), corrosion current density, (i_{corr}), anodic and cathodic Tafel slopes (β_a, β_c), for zinc in 0.5 mol·L^{-1} citric acid with different DTPB

Tab. 1 The inhibition efficiency (*IE*) for the corrosion of zinc in 0.5 mol·L^{-1} citric acid free from and containing 10^{-5} and 10^{-4} mol·L^{-1} DTPB in the absence and presence of 10^{-3} mol·L^{-1} KI obtained from weight loss measurements at 30 ℃

Solution	*IE*/%				
	12 h	24 h	48 h	72 h	96 h
0.5 mol·L^{-1} citric acid + 10^{-3} mol·L^{-1} KI	22.9	22.0	19.2	16.1	14.7
0.5 mol·L^{-1} citric acid + 10^{-5} mol·L^{-1} DTPB	40.6	39.8	38.8	37.5	36.1
0.5 mol·L^{-1} citric acid + 10^{-5}mol·L^{-1} DTPB + 10^{-3} mol·L^{-1} KI	76.6	75.0	72.2	70.9	69.1
0.5 mol·L^{-1} citric acid + 10^{-4} mol·L^{-1} DTPB	67.1	65.5	62.8	60.0	58.2
0.5 mol·L^{-1} citric acid + 10^{-4} mol·L^{-1} DTPB + 10^{-3} mol·L^{-1} KI	99.4	99.3	98.6	98.3	97.6

Fig. 3 Photographs of zinc panels after three hours of immersion in different citric acid solutions
A. 0.5 mol·L^{-1} citric acid; B. 0.5 mol·L^{-1} citric acid + 10^{-3} mol·L^{-1} KI; C. 0.5 mol·L^{-1} citric acid + 10^{-4} mol·L^{-1} DTPB; D. 0.5 mol·L^{-1} citric acid + 10^{-4} mol·L^{-1} DTPB+ 10^{-3} mol·L^{-1} KI

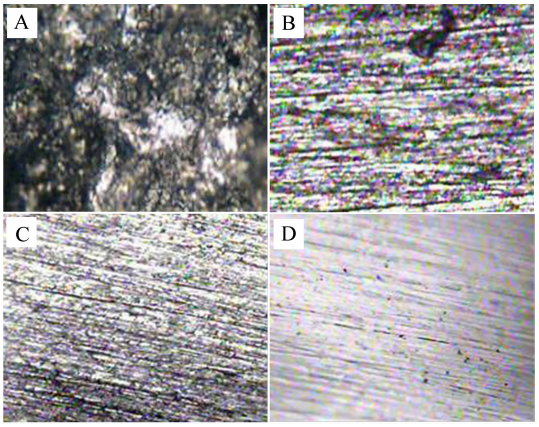

Fig. 4 Optical microscopic photos (40 ×) for zinc submerged for 24 h in 0.5 mol·L^{-1} citric acid free from and containing 10^{-5} mol·L^{-1} DTPB in the absence and presence of 10^{-3} mol·L^{-1} KI
A. 0.5 mol·L^{-1} citric acid; B. 0.5 mol·L^{-1} citric acid + 10^{-3} mol·L^{-1} KI; C. 0.5 mol·L^{-1} citric acid + 10^{-4} mol·L^{-1} DTPB; D. 0.5 mol·L^{-1} citric acid + 10^{-4} mol·L^{-1} DTPB+ 10^{-3} mol·L^{-1} KI

concentrations are presented in Tab. 2.

The data in Tab. 2 demonstrate that increasing the DTPB concentration decreased the values of i_{corr} and slightly shifted the values of E_{corr} to a more positive direction, which probably means that the addition of DTPB causes the zinc surface to behave as a noble metal. This might be caused by the formation of the strong adsorption layer which protects the Zn surface from corrosion[38]. The slight variations in values of β_a indicate that the inhibiting action in an anodic dissolution of a metal took place by the simple blocking of the available anodic sites of the surface, while the appreciable changes in the values of β_c indicate that DTPB affected the mechanism of the cathodic reaction, which is a proton discharge step[42]. Fig. 6 illustrates the potentiodynamic polarization curves for zinc in 0.5 mol·L^{-1} citric acid solution in the absence and presence of different KI concentrations at 30 ℃.

It is clear from Fig. 6 that the addition of KI affected only the anodic part of the polarization curve, indicating that it could be classified as anodic-type inhibitor. The electrochemical polarization parameters for zinc in 0.5 mol·L^{-1} citric acid solution in the absence and presence of different KI concentrations are presented in Tab. 3.

As evident in Tab. 3, increasing KI concentration decreased the values of i_{corr} and slightly shifted the values of E_{corr} to a more positive direction. The values of β_a and β_c were slightly changed, indicating that KI caused simple blocking of anodic and cathodic sites on the metal surface. Fig. 7 shows the potentiodynamic polarization curves of zinc in 0.5 mol·L^{-1} citric acid solution, free from and containing 10^{-3} mol·L^{-1} KI, 10^{-5} mol·L^{-1} DTPB, and both 10^{-3} mol·L^{-1} KI + 10^{-5} mol·L^{-1} DTPB at 30 ℃.

It is clear from Fig. 7 that the presence of DTPB or KI shifted the corrosion potentials to more positive values and in the presence of both of them, the corrosion potential also shifted to more positive values.

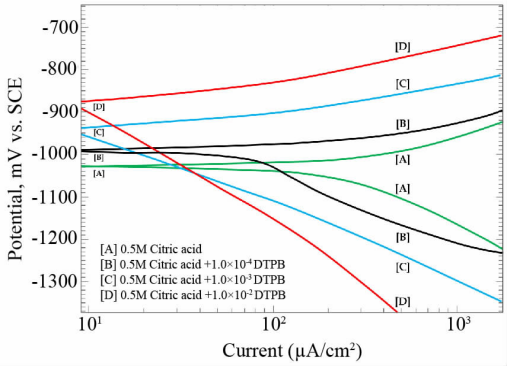

Fig. 5 Potentiodynamic polarization curves for zinc in 0.5 mol·L^{-1} citric acid in the absence and presence of different DTPB concentrations at 30 ℃

Tab. 2 Electrochemical polarization parameters of zinc in 0.5 mol·L^{-1} citric acid with different DTPB concentrations at 30 ℃

C/(mol·L^{-1})	$-E_{corr}$/mV(vs. SCE)	β_a/(mV·decade^{-1})	$-\beta_c$/(mV·decade^{-1})	i_{corr}/(mm·year^{-1})	IE/%
0	1035	94	140	2.62	-
$1.0\cdot10^{-5}$	997	95	235	1.64	37.1
$2.5\cdot10^{-5}$	993	100	238	1.39	46.8
$5.0\cdot10^{-5}$	989	88	243	1.23	53.1
$7.5\cdot10^{-5}$	984	85	247	1.019	61.1
$1.0\cdot10^{-4}$	980	94	248	0.880	66.2
$2.5\cdot10^{-4}$	973	85	251	0.644	75.4
$5.0\cdot10^{-4}$	967	81	255	0.464	82.3
$7.5\cdot10^{-4}$	962	93	262	0.329	87.4
$1.0\cdot10^{-3}$	955	82	272	0.225	91.4
$2.5\cdot10^{-3}$	944	80	292	0.105	96.0
$3.0\cdot10^{-3}$	937	88	272	0.030	98.9

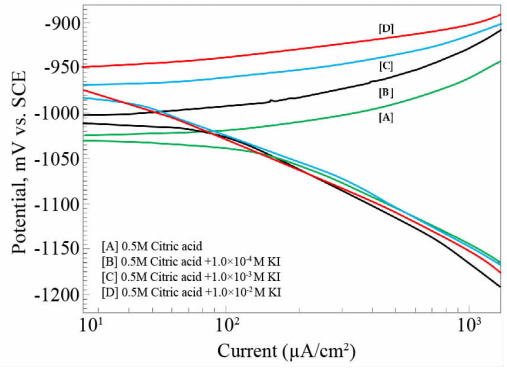

Fig. 6 Potentiodynamic polarization curves of zinc in 0.5 mol·L^{-1} citric acid solution in the absence and presence of different KI concentrations at 30 ℃

The anodic branches shifted to a more positive potential direction, while the cathodic branches shifted to a more negative potential direction, which indicates that the combination of DTPB and KI acted as a mixed type inhibitor. The values of the electrochemical parameters for zinc in 0.5 mol·L^{-1} citric acid solution, free from and containing 10^{-3} mol·L^{-1} KI, 10^{-5} mol·L^{-1} DTPB, and both 10^{-3} mol·L^{-1} KI + 10^{-5} mol·L^{-1} DTPB are presented in Tab. 4.

The data in Tab. 4 indicate that the values of i_{corr} were markedly depressed in the presence of the DTPB and KI combination, which may be explained on the basis of synergism between the KI and DTPB molecule.

2.5 Electrochemical Impedance Spectroscopic Analysis

The Nyquist plots of zinc in 0.5 mol·L^{-1} citric acid containing different DTPB concentrations at 30 ℃ are compared in Fig. 8. Depressed semicircles of a capacitive type were observed, indicating that the dissolution process occured under activation control.

Tab. 3 The electrochemical polarization parameters for zinc in 0.5 mol·L^{-1} citric acid solution in the absence and presence of different KI concentrations at 30 ℃

Solution	$-E_{corr}$/(mV·SCE^{-1})	β_a/(mV·decade^{-1})	$-\beta_c$/(mV·decade^{-1})	i_{corr}/(mm·year^{-1})	IE/%
0.5 mol·L^{-1} citric acid	1035	94	140	2.62	-
0.5 mol·L^{-1} citric acid + 10^{-4} mol·L^{-1} KI	1030	95	208	2.26	13.7
0.5 mol·L^{-1} citric acid + 10^{-3} mol·L^{-1} KI	1025	90	229	2.097	20.0
0.5 mol·L^{-1} citric acid + 10^{-2} mol·L^{-1} KI	1010	100	235	1.68	36.0

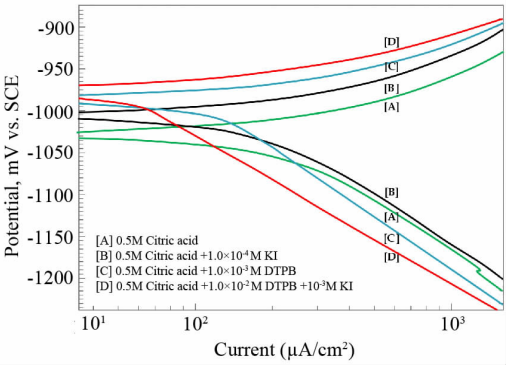

Fig. 7 Potentiodynamic polarization curves of zinc in 0.5 mol·L^{-1} citric acid solution, free from and containing 10^{-3} mol·L^{-1} KI, 10^{-5} mol·L^{-1} DTPB, and both 10^{-3} mol·L^{-1} KI + 10^{-5} mol·L^{-1} DTPB at 30 ℃

The size of the semicircles increased with increasing concentration of the inhibitor. Fig. 9 shows that the impedance responses of zinc in citric acid in the absence and presence of different concentrations of DTPB had one time constant.

The impedance spectra for different Nyquist plots were analyzed by fitting the experimental data into the equivalent circuit model (Fig. 10), that includes the solution resistance (R_s) and constant phase element of the double layer (CPE_{dl}) which is placed in parallel to charge transfer resistance element, R_{ct}. The fitting results are also included in Fig. 8 and Fig. 9 as solid lines.

The R_{ct} value is a measure of electron transfer across the surface and is inversely proportional to corrosion rate. The capacitances were implemented as a constant phase element (CPE) during the analysis of the impedance plots. The CPE is defined by two values, Q and n. The impedance, Z, of CPE is presented by:

$$Z_{CPE} = Q^{-1}(j\omega)^{-n} \quad (2)$$

where $j = (-1)^{1/2}$, ω is angular frequency, $\omega = 2\pi f$ and f is the frequency. If n equals one, then Eq. (2) is identical to that of a capacitor, $Z_{CPE} = (j\omega C)^{-1}$ where C is the ideal capacitance. For a non-homogeneous system, n values range from 0.9 to 1. The values of R_{ct} and Q_{dl} for zinc in 0.5 mol·L^{-1} citric acid containing different DTPB concentrations are presented in Fig. 11.

The data in Fig. 11 indicate that the increase in the concentration of DTPB led to increasing the charge transfer resistance that is associated with a decrease in Q_{dl}. Hence, the double layer capacitance can be expressed in the Helmholtz model by:

$$C_{dl} = \varepsilon\varepsilon_0\left(\frac{A}{d}\right) \quad (3)$$

where "d" is the thickness of electrical double layer, A is the surface of the electrode, ε_0 is the permittivity of vacuum and ε is the medium dielectric constant[43]. Therefore, the decrease in C_{dl} or Q_{dl} could be related to the decrease of the local dielectric constant (ε) or increase of thickness of the electrical double layer due to the formation of a protective layer by the adsorption of inhibitor molecules on the metal surface[44-45]. Fig. s 12, 13 demonstrate the Nyquist and bode plots of zinc in 0.5 mol·L^{-1} citric acid solution, free from and containing 10^{-3} mol·L^{-1} KI, 10^{-5} mol·L^{-1} DTPB, and both 10^{-3} mol·L^{-1} KI + 10^{-5} mol·L^{-1} DTPB at 30 ℃, respectively. The bode plots had only one time constant. The impedance spectra for the Nyquist plots were analyzed by fitting the experimental data to the same equivalent circuit model (Fig. 10.)

Tab. 4 The values of the electrochemical parameters for zinc in 0.5 mol·L^{-1} citric acid solution, free from and containing 10^{-3} mol·L^{-1} KI, 10^{-5} mol·L^{-1} DTPB, and both 10^{-3} mol·L^{-1} KI + 10^{-5} mol·L^{-1} DTPB at 30 ℃

Solution	$-E_{corr}$/ mV(vs. SCE)	β_a/ (mV·decade^{-1})	$-\beta_c$/ (mV·decade^{-1})	i_{corr}/ (mm·year^{-1})	*IE*/%
0.5 mol·L^{-1} citric acid	1035	94	140	2.62	-
0.5 mol·L^{-1} citric acid + 10^{-3} mol·L^{-1} KI	1025	91	229	2.097	20.0
0.5 mol·L^{-1} citric acid + 10^{-5} mol·L^{-1} DTPB	997	95	235	1.65	37.1
0.5 mol·L^{-1} citric acid + 10^{-5}mol·L^{-1} DTPB + 10^{-3} mol·L^{-1} KI	985	87	235	0.839	68.0

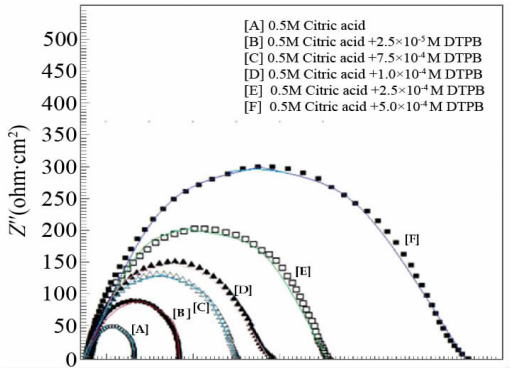

Fig. 8 Nyquist plots of zinc in 0.5 mol·L^{-1} citric acid containing different DTPB concentrations at 30 ℃

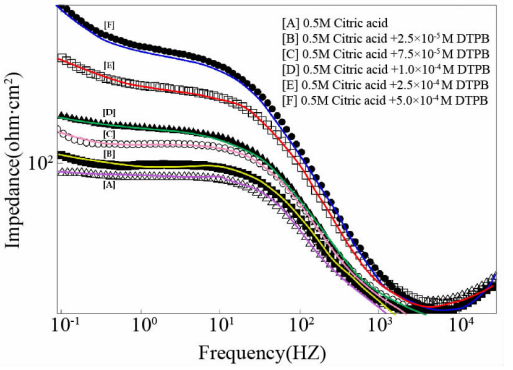

Fig. 9 Bode plots of zinc in 0.5 mol·L^{-1} citric acid containing different DTPB concentrations at 30 ℃

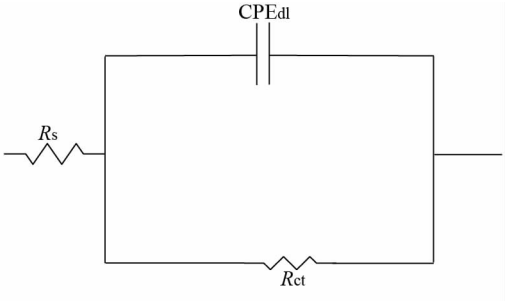

Fig. 10 The suggested equivalent circuit

The values of R_{ct} and Q_{dl} for zinc in 0.5 mol·L^{-1} citric acid solution, free from and containing 10^{-3} mol·L^{-1} KI, 10^{-5} mol·L^{-1} DTPB, and both 10^{-3} mol·L^{-1} KI and 10^{-5} mol·L^{-1} DTPB are presented in Tab. 5. Apparently, the addition of KI to 0.5 mol·L^{-1} citric acid solutions containing DTPB further enhanced R_{ct} values and reduced Q_{dl} values. In accordance, the inhibition efficiencies increased markedly in the presence of DTPB and KI combination, indicating that a

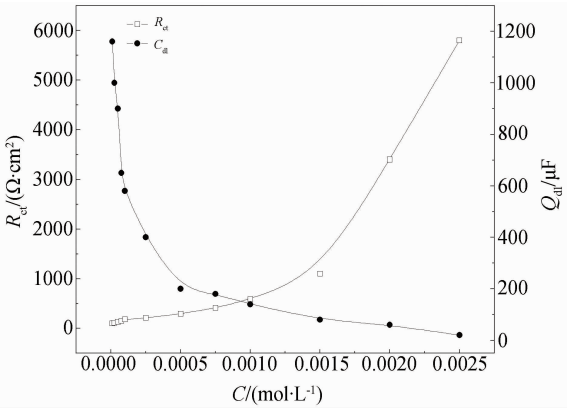

Fig. 11 Variations of R_{ct} and Q_{dl} values for zinc in 0.5 mol·L^{-1} citric acid containing different DTPB concentrations

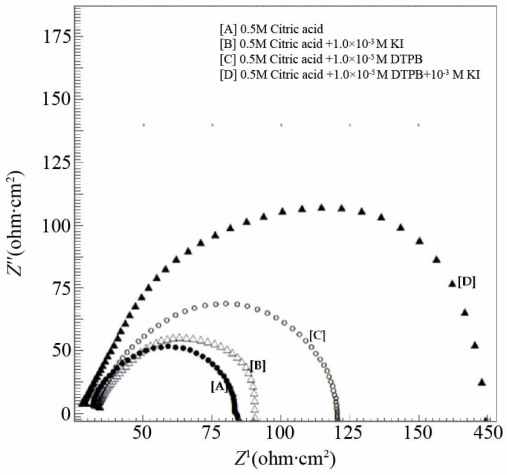

Fig. 12 Nyquist plots of zinc in 0.5 mol·L^{-1} citric acid solution, free from and containing 10^{-3} mol·L^{-1} KI, 10^{-5} mol·L^{-1} DTPB, and both 10^{-3} mol·L^{-1} KI + 10^{-5} mol·L^{-1} DTPB at 30 ℃

substantial synergistic improvement in the inhibition efficiency of DTPB was observed in the presence of KI.

2.6 Application of Adsorption Isotherms

The degree of surface coverage (θ) of the metal surface by an adsorbed inhibitor is calculated from impedance measurements using the equation[46]:

$$\frac{C_{dl}}{C_{dl_o}} = \frac{1-\theta}{1} \quad (4)$$

where C_{dl_o} and C_{dl} are the double layer capacitance for zinc in 0.5 mol·L^{-1} citric acid in the absence and presence of an inhibitor solution, respectively. The variation of surface coverage with the concentration of

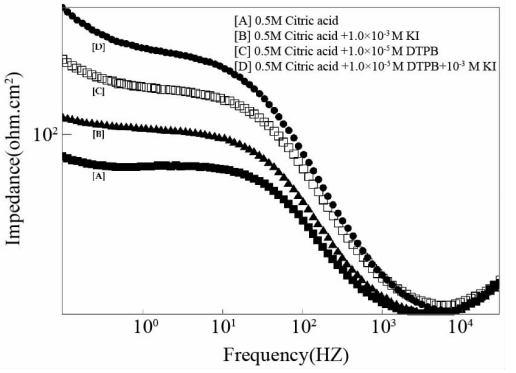

Fig. 13 Bode plots of zinc in 0.5 mol·L^{-1} citric acid solution, free from and containing 10^{-3} mol·L^{-1} KI, 10^{-5} mol·L^{-1} DTPB, and both 10^{-3} mol·L^{-1} KI + 10^{-5} mol·L^{-1} DTPB at 30 ℃

DTPB is illustrated in Fig. 14.

The adsorption curve, Fig. 14, represents an adsorption isotherm that is characterized by the first sharp rising part followed by another gradual rising part, indicating the formation of a mono-layer adsorbate film on the zinc surface.

The Langmuir isotherm is given by reference[47].

$$\left(\frac{\theta}{1-\theta}\right) = KC \tag{5}$$

where K is the binding constant representing the interaction of the additives with the metal surface and C is the concentration of the additives.

Flory-Huggins isotherm is given by reference[48]:

$$\frac{\theta}{x(1-\theta)^{x}} = KC \tag{6}$$

where x is the size parameter, a measure of the number of adsorbed water molecules substituted by a given inhibitor molecule.

The kinetic-thermodynamic model is given by reference[49]:

$$\lg\left(\frac{\theta}{1-\theta}\right) = \lg K' + y\lg C \tag{7}$$

where y is the number of inhibitor molecules occupying one active site. The binding constant K is given by: $K = K'^{(1/y)}$ (8)

The previously mentioned isotherms were used to fit the corrosion data of the inhibitor solutions. The parameters obtained from these Figures are presented in Tab. 6.

Langmuir isotherm was found to be not applicable to fit the corrosion data of DTPB, indicating that there might be a non-ideal behavior in the adsorption process of DTPB on the zinc surface[50], but fitted the corrosion data of KI or the combination of DTPB and KI. Since the values of the size parameter x are larger than 1 (Tab. 6) in the presence of DTPB, which indicates that the adsorbed species of DTPB could displace more than one water molecule from the zinc surface. On the other hand, only one active site was displaced in the presence of KI or the combination of DTPB and KI. The numbers of active sites occupied by a single inhibitor molecule, $1/y$, are nearly equal to the size parameter x. The binding constant values (K) for the combination of DTPB and KI are greater than those for DTPB or KI confirming the suggested synergistic effect between KI and DTPB molecule. The approximately identical binding constant values (K) obtained in the presences of KI and combination of KI and DTPB indicate a fairly good agreement between the Langmuir, Flory-Huggins isotherm and the kinetic thermodynamic model.

2.7 Calculation of Synergism Parameter

The synergism parameter, S, was evaluated using the relationship below, as was reported in a previous work[51]:.

Tab. 5 The values of R_{ct} and Q_{dl} for zinc in 0.5 mol·L^{-1} citric acid solution, free from and containing 10^{-3} mol·L^{-1} KI, 10^{-5} mol·L^{-1} DTPB, and both 10^{-3} mol·L^{-1} KI + 10^{-5} mol·L^{-1} DTPB at 30 ℃

Solution	C_{dl}/μF	R_{ct}/(Ω·cm^2)	IE/%
0.5 mol·L^{-1} citric acid	127	53	-
0.5 mol·L^{-1} citric acid +10^{-3} mol·l^{-1} KI	104	69	23.2
0.5 mol·L^{-1} citric acid + 10^{-5} mol·l^{-1} DTPB	93	85	37.6
0.5 mol·L^{-1} citric acid +10^{-5} mol·L^{-1} DTPB + 10^{-3} mol·L^{-1} KI	65	195	72.8

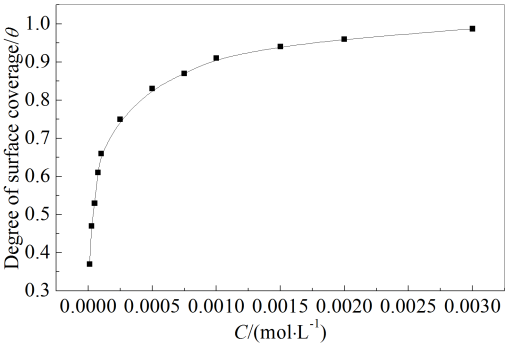

Fig. 14 Variation of surface coverage with the concentration of DTPB at 30 ℃

$$S = \frac{1\text{-}I_{12}}{1\text{-}I_1\text{-}I_2} \tag{9}$$

where I_1 is the inhibition efficiency of iodide ion, I_2 is the inhibition efficiency of DTPB, and I_{12} is the measured inhibition efficiency for DTPB in combination with iodide ion. The values of S = 1.21, 1.19 and 1.20 are calculated from the data of the weight loss (Tab. 1), potentiodynamic polarization (Tab. 4), and impedance (Tab. 5), respectively. The value of S, greater than the unit, is an indication that the enhanced inhibition efficiency, resulting from the addition of iodide ion to DTPB, is synergistic in nature.

2.8 Inhibition Mechanism

It has been reported[38] that the specific adsorption of iodide assisted the inhibitory effect of an organic molecule on the surface of zinc and halide ions are typically well adsorbed on the metal surfaces[51]. Chemisorbed ions enter the charged metal surfaces which are positively charged in the presence of an acidic medium[38], while halide ions are negatively charged, the specific adsorption of halide ions onto the zinc surface results in a negatively charged zinc surface by means of electrostatic or coulombic attraction. This process is similar to the phenomenon so called anion induced adsorption and may be represented by the following highly simplified mechanism[52-53].

$$X_s \rightarrow X_{ads} \tag{10}$$

$$M_s + X_{ads} \rightarrow MX_{ads} \tag{11}$$

where X_s and M_s designate the halide ion and organic species, respectively, in the bulk state, X_{ads} and MX_{ads} refer to a halide and ion pair, respectively, in the adsorbed state.

According to this mechanism, the ionized DTPB easily reaches the zinc surface, and the dipoles of the surface compound are oriented with their negative ends towards the solution. This ion pair interaction consequently increases the surface coverage preventing the acid solution from attaching directly to zinc surface, thereby, reducing metal dissolution. Therefore, it can be deduced that iodide ion acts as an adsorption mediator for bonding the metal surface and DTPB or iodide ions are sandwiched between the metal and a positively charged part of the inhibitor, and this may be responsible for the synergistic effect of the iodide ion on DTPB. This is strongly confirmed by the y values obtained from the kinetic-thermodynamic model which represents the number of inhibitor molecules occupying one active site, since its value in the presence of KI alone is similar to that in the presence of a combination of KI and DTPB. It was suggested that in both cases, iodide ion is adsorbed at the surface assisting a stronger adsorption of the DTPB molecule also at the surface, while in the presence of DTPB alone, the y value is greater than 1 due to the adsorption of the bulky DTPB molecules at the surface which cover more than one active center, but it is not strongly bound to the surface since it has a small binding constant. The combination of DTPB and KI has a larger binding constant

Tab. 6 Linear fitting parameters of DTPB according to the applied models

	Langmuir	Flory- Huggins		Kinetic-Thermodynamic	
Solution	K	x	K	$1/y$	K
0.5 mol·L^{-1} citric acid + 10^{-3} mol·L^{-1} KI	2800	0.99	3100	1.04	2900
0.5 mol·L^{-1} citric acid + 10^{-5} mol·L^{-1} DTPB	-	2.80	610	0.38	550
0.5 mol·L^{-1} citric acid +10^{-5} mol·L^{-1} DTPB + 10^{-3} mol·L^{-1} KI	33000	1.03	27000	0.95	31000

and, therefore, the DTPB molecule and iodide ion are strongly adsorbed at the surface. Furthermore, this confirms that KI acts as an adsorption mediator for bonding metal surface and DTPB.

2.9 Spectrophotometric UV Results

Fig. 15 illustrates the UV-Visible spectra in the solutions of 0.5 mol·L^{-1} citric acid containing 10^{-3} mol·L^{-1} Zn^{2+} ions, 0.5 mol·L^{-1} citric acid containing 10^{-3} mol·L^{-1} Zn^{2+} ions with 10^{-4} mol·L^{-1} DTPB and 0.5 mol·L^{-1} citric acid containing 10^{-3} mol·L^{-1} Zn^{2+} ions with 10^{-3} mol·L^{-1} KI. Fig. 16 shows the UV-Visible spectrum in the solution of 0.5 mol·L^{-1} citric acid containing 10^{-3} mol·L^{-1} Zn^{2+} ions with both 10^{-4} mol·L^{-1} DTPB and 10^{-3} mol·L^{-1} KI.

The λ_{max} values of bands characteristic for each solution are listed in Tab. 7. Both Fig. 15 and Tab. 7 show that the three solutions exhibited the same absorption band at 218 nm corresponding to citric acid. The solution containing DTPB with citric acid exhibited an additional band at 265 nm that corresponds to the presence of DTPB, while the solution containing citric acid and KI exhibited two bands at 284 and 349 nm corresponding to the liberated I_2 formed. Fig. 16 and Tab. 7 show that when both KI and DTPB are present in citric acid, the two bands corresponding to I_2 disappear completely, indicating that iodide ion existed in a bonded form with a slight shift of the DTPB band from 265 to 275 nm, confirming the above mentioned inhibition mechanism.

2.10 Synergistic Effect between KI and DTPB at Different Temperatures

The inhibition efficiency and synergism parameter calculated at different temperatures by utilizing EIS technique for different solutions are presented in Tab. 8. The displayed data in Tab. 8 indicate that both the inhibition efficiency of the inhibitor solutions for zinc in 0.5 mol·L^{-1} citric acid and the synergism parameter between KI and DTPB slightly decreased as the temperature was raised up to 55 ℃. An appreciable decrease in the inhibition efficiency was observed at 56 ℃, moreover, the synergism parameter approached 1, thus, the synergistic effect between KI and DTPB was considered only up to 55 ℃. The decrease in the inhibition efficiency of inhibitors with temperature may be attributed to the weakness of physical bonds formed due to the adsorption of intermediate iodide ion at the zinc surface at high temperature.

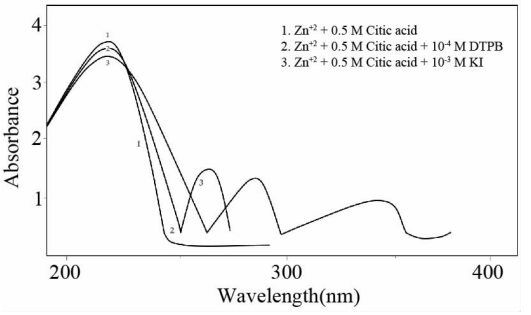

Fig. 15 UV-Visible spectra in different citric acid solutions

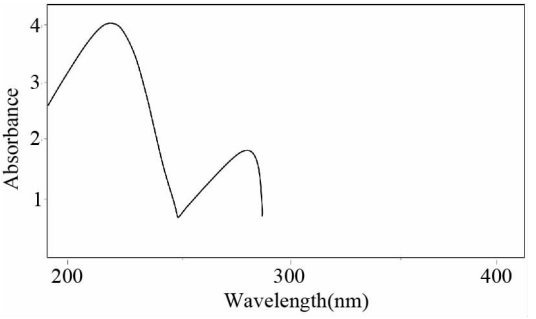

Fig. 16 UV-Visible spectrum in the solution of 0.5 mol·L^{-1} citric acid containing 10^{-3} mol·L^{-1} Zn^{2+} ions with both 10^{-4} mol·L^{-1} DTPB and 10^{-3} mol·L^{-1}KI

Tab. 7 List of λ_{max} for different bands characteristic in different solutions

Solution	λ_{max}/nm		
0.5 mol·L^{-1} citric acid + 10^{-3} mol·L^{-1} Zn^{+2}	218	-	-
0.5 mol·L^{-1} citric acid + 10^{-3} mol·L^{-1} Zn^{+2} + 10^{-4} mol·L^{-1} DTPB	218	265	-
0.5 mol·L^{-1} citric acid + 10^{-3} mol·L^{-1} Zn^{+2} + 10^{-3} mol·L^{-1} KI	218	284	349
0.5 mol·L^{-1} citric acid + 10^{-3} mol·L^{-1} Zn^{+2} + 10^{-4} mol·L^{-1} DTPB+10^{-3} mol·L^{-1} KI	218	270	-

Tab. 8 The inhibition efficiency and synergism parameter calculated at different temperatures using EIS technique for different solutions

Solution	*IE* at different temperatures/%					
	30 ℃	40 ℃	50 ℃	55 ℃	56 ℃	57 ℃
0.5 mol·L^{-1} citric acid +10^{-3} mol·L^{-1} KI	22.8	22.2	21.8	20.3	19.5	19.0
0.5 mol·L^{-1} citric acid + 10^{-5} mol·L^{-1} DTPB	38.0	37.0	36.4	35.0	34.4	33.8
0.5 mol·L^{-1} citric acid +10-5 mol·L^{-1} DTPB + 10^{-3} mol·L^{-1} KI	72.8	69.8	67.6	63.7	56.0	54.4
S (Synergism parameter)	1.20	1.18	1.16	1.15	1.04	1.03

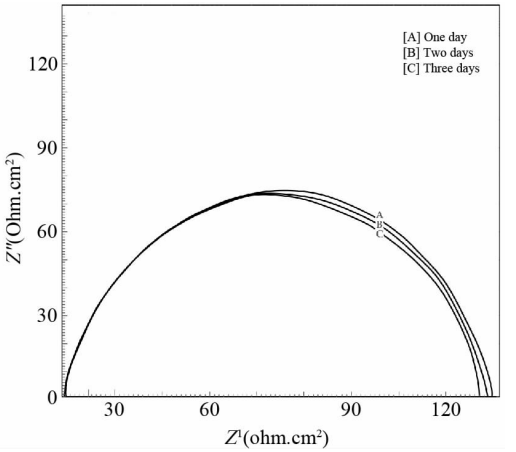

Fig. 17 Nyquist plots of zinc in 0.5 mol·L^{-1} citric acid containing 10^{-5} mol·L^{-1} DTPB at 30 ℃ after different exposure time

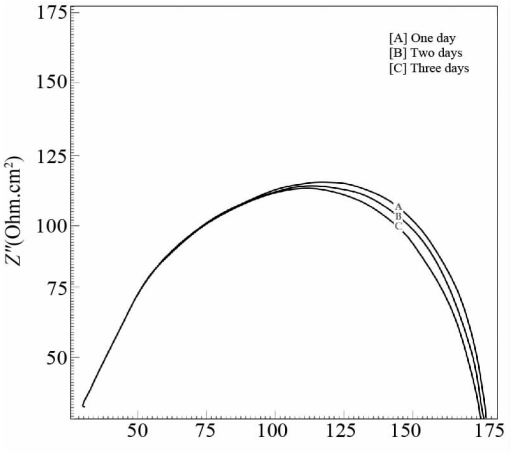

Fig. 18 Nyquist plots of zinc in 0.5 mol·L^{-1} citric acid containing both 10^{-3} mol·L^{-1} KI and 10^{-5} mol·L^{-1} DTPB at 30 ℃ after different exposure time

2.11 Synergistic Effect between KI and DTPB at Different Exposure Time

Figs. 17, 18 demonstrate the Nyquist plots of zinc in 0.5 mol·L^{-1} citric acid in the presences of 10^{-5} mol·L^{-1} DTPB and 10^{-5} mol·L^{-1} DTPB with the addition of 10^{-3} mol·L^{-1} KI, respectively, at 30 ℃ after different exposure time. The inhibition efficiency of DTPB and synergism between KI and DTPB slightly decreased after three days of exposure, confirming the great inhibition efficiency of DTPB and the efficient synergistic effect of KI for zinc corrosion in citric acid.

3 Conclusions

It was found that (1,3-dioxolan-2-ylmethyl)-triphenylphosphonium bromide (DTPB) could act as an effective corrosion inhibitor for zinc corrosion in citric acid. The inhibiting action of DTPB was attributed to its adsorption over the metal surface that blocks the available cathodic and anodic sites. Synergism between the KI and DTPB molecule was valid only up to 55 ℃. Adsorption isotherms indicated that the adsorbed DTPB molecule covered more than one active center over the metal surface, but it was not strongly held to the surface as indicated by the small binding constant, while the combination between DTPB and KI covered one active center with strong adsorption at the surface (larger binding constant), indicating that KI acted as an adsorption mediator for bonding metal surface and DTPB.

Acknowledgement

The work was supported by Corrosion Laboratory, Chemistry department, Faculty of science, Alexandria university, Egypt. The author wishes to thank Prof. Dr. Beshir Ahmed Abd El-Nabey, Prof. Dr. Essam Khamis and Prof. Dr. Ashraf Moustafa, Department of chemistry, Faculty of Science, Alexandria University, Alexandria, Egypt for continuous sup-

port and providing advanced instruments.

References:

[1] Hardesty F. Metals Handbook, Properties and Selection: Nonferrous alloys and pure metals[M]. vol 2, 9th ed., (ASM, USA, Elsevier B.V. 1981): 249.

[2] Zhou H B, Huang Q M, Liang M, et al. Investigation on synergism of composite additives for zinc corrosion inhibition in alkaline solution[J]. Materials Chemistry and Physics, 2011, 128(1): 214-219.

[3] Liu S, Zhong Y, Jiang R, et al. Corrosion inhibition of zinc in tetra-n-butylammonium bromide aerated aqueous solution by benzotriazole and Na_3PO_4[J]. Corrosion Science, 2011, 53(2): 746-759.

[4] Aramaki K. Synergistic inhibition of zinc corrosion in 0.5 M NaCl by combination of cerium(III) chloride and sodium silicate[J]. Corrosion Science, 2002, 44(4): 871-886.

[5] Georges C, Rocca E, Steinmetz P. Synergistic effect of tolutriazol and sodium carboxylates on zinc corrosion in atmospheric conditions[J]. Electrochimica Acta, 2008, 53(14): 4839-4845.

[6] Pruna A, Pilan L. Electrochemical study on new polymer composite for zinc corrosion protection[J]. Composites Part B: Engineering, 2012, 43(8): 3251-3257.

[7] Qiu R, Zhang D, Wang P. Superhydrophobic-carbon fibre growth on a zinc surface for corrosion inhibition[J]. Corrosion Science, 2013, 66(1): 350-359.

[8] Aghzzaf A A, Rhouta B, Rocca E, et al. Corrosion inhibition of zinc by calcium exchanged beidellite clay mineral: A new smart corrosion inhibitor[J]. Corrosion Science, 2014, 80(1): 46-52.

[9] Muller B, Inblo G. Heterocycles as corrosion inhibitors for zinc pigments in aqueous alkaline media[J]. Corrosion Science, 1996, 38(2): 293-300.

[10] Foad El-Sherbini E E, Abdel Wahaab S M, Deyab M. Ethoxylated fatty acids as inhibitors for the corrosion of zinc in acid media[J]. Materials Chemistry and Physics, 2005, 89(2): 183-191.

[11] Basio F, Poarson R G. Mechanism of Inorganic Reaction, second ed.[M]. John Wiley, London, 1967.

[12] Abdallah M. Ethoxylated fatty alcohols as corrosion inhibitors for dissolution of zinc in hydrochloric acid[J]. Corrosion Science, 2003, 45(12): 2705-2716.

[13] Abdel Aal M S, Ahmed Z A, Hassan M S. Inhibiting and accelerating effects of some quinolines on the corrosion of zinc and some binary zinc alloys in HCl solution[J]. Journal of Applied Electrochemistry, 1992, 22(11): 1104-1109.

[14] Talati J D, Desai M N, Shah N K. Meta-substituted aniline-N-salicylidenes as corrosion inhibitors of zinc in sulphuric acid[J]. Materials Chemistry and Physics, 2005, 93 (1): 54-64.

[15] Agrawal Y K, Talati J D, Shah M D, et al. Schiff bases of ethylenediamine as corrosion inhibitors of zinc in sulphuric acid[J]. Corrosion Science, 2004, 46(3): 633-651.

[16] Mihit M, Laarej K, Abou El Makarim H, et al. Study of the inhibition of the corrosion of copper and zinc in HNO_3 solution by electrochemical technique and quantum chemical calculations[J]. Arabian Journal of Chemistry, 2010, 3(1): 55-60.

[17] Wang L, Pu J X, Luo H C. Corrosion inhibition of zinc in phosphoric acid solution by 2-mercaptobenzimidazole[J]. Corrosion Science, 2003, 45(4): 677-683.

[18] Morad M S. Inhibition of phosphoric acid corrosion of zinc by organic onium compounds and their adsorption characteristics[J]. Journal of Applied Electrochemistry, 1999, 29(5): 619-626.

[19] Rudresh H B, Mayanna S M. Role of the thiocyanate ion in the corrosion inhibition of zinc in perchloric acid by *n*-decylamine[J]. Surface Technology, 1979, 8(3): 185-194.

[20] Shanming H, Wang J, Yan J. Pressure leaching of synthetic zinc silicate in sulfuric acid medium[J]. Hydrometallurgy, 2011, 108(3/4): 171-176.

[21] Hosary AAE, Saleh R M, Din AMSE. Corrosion inhibition by naturally occurring substances[J]. Corrosion Science, 1972, 12(12): 897-904.

[22] Abiola O K, James A O. The effects of Aloe vera extract on corrosion and kinetics of corrosion process of zinc in HCl solution[J]. Corrosion Science, 2010, 52(2): 661-664.

[23] Hosseini M, Mertens S F L, Arshadi M R. Synergism and antagonismin of mild steel corrosion inhibition by sodium dodecyl benzene sulphonate and hexamethylenetetramine[J]. Corrosion Science, 2003, 45(7): 1473-1489.

[24] Li X M, Tang L B, Li L et al. Synergistic inhibition between o-phenanthroline and chloride ion for steel corrosion in sulphuric acid[J]. Corrosion Science, 2006, 48(2): 308-321.

[25] Li X H, Deng S D, Fu H. Synergistic inhibition effect of red tetrazolium and uracil on the corrosion of cold rolled steel in H_3PO_4 solution: Weight loss, electrochemical, and AFM approaches[J]. Materials Chemistry and Physics, 2009, 115(2/3): 815-824.

[26] Solmaz R, Sahin E A, Döner A, et al. The investigation of synergistic inhibition effect of rhodamine and iodide ion on the corrosion of copper in sulphuric acid solution[J].

Corrosion Science, 2011, 53(10): 3231-3240.

[27] Heydari M, Javidi M. Corrosion inhibition and adsorption behaviour of an amido-imidazolinederivative on API 5L X52 steel in CO_2-saturated solution and synergistic effect of iodide ions[J]. Corrosion Science, 2012, 61(1): 148-155.

[28] Godec R F, Pavlovic M G. Synergistic effect between non-ionic surfactant and halide ions in the forms of inorganic or organic salts for the corrosion inhibition of stainless-steel X4Cr13 in sulphuric acid[J]. Corrosion Science, 2012, 58(1): 192-201.

[29] Khamis A, Saleh M M, Awad M I. Synergistic inhibitor effect of cetylpyridinium chloride and other halides on the corrosion of mild steel in 0.5 mol·L^{-1} H_2SO_4[J]. Corrosion Science, 2013, 66(1): 343-349.

[30] Gunasekaran G, Palanisamy N, Appa Raob B V, et al. Synergistic inhibition in low chloride media[J]. Electrochimica Acta, 1997, 42(9): 1427-1434.

[31] Rudresh H B, Mayanna S M. The synergistic effect of halide ions on the corrosion inhibition of zinc by n-decylamine[J]. Corrosion Science, 1979, 19(6): 361-370.

[32] Saeki I, Seguchi T, Kourakat Y et al. Ni electroplating on AZ91D Mg alloy using alkaline citric acid bath[J]. Electrochimica Acta, 2013, 114(1): 827-831.

[33] Bastidas J M, Scantlebury J D. The influence of light on corrosion phenomena: The behaviour of mild steel in citric acid solution[J]. Corrosion Science, 1986, 26(5): 341-347.

[34] Rehim S S A, Sayyah S M, El Deeb M M. Corrosion of tin in citric acid solution and the effect of some inorganic anions[J]. Materials Chemistry and Physics, 2003, 80(3): 696-703.

[35] Jafrian M, Gobal F, Danaai I, et al. Electrochemical studies of the pitting corrosion of tin in citric acid solution containing chloride[J]. Electrochimica Acta, 2008, 53(13): 4528-4536.

[36] Zerfaoui M, Oudda H, Hammouti B, et al. Inhibition of corrosion of iron in citric acid media by aminoacids[J]. Progress in Organic Coatings, 2004, 51(2): 134-138.

[37] El-Gaber A S, Fouda A S, El Desoky A M. Synergistic inhibition of zinc corrosion by some anions in aqueous media[J]. Ciência&Tecnologia dos Materiais, 2008, 20 (3/4): 71-77.

[38] Li X H, Deng S D, Xie X G, et al. Inhibition effect of bamboo leaves extract on steel and zinc in citric acid solution[J]. Corrosion Science, 2014, 87(1): 15-26.

[39] Larba R, Boukerche I, Alane N, et al. Citric acid as an alternative lixiviant for zinc oxide dissolution[J]. Hydrometallurgy, 2013, 134: 117-123.

[40] Cresp T M, Sargent M V, Vogel P J C S[J]. A synthesis of $\alpha\beta$-unsaturated aldehydes. Journal of the Chemical Society, Perkin Transactions 1, 1974, 37-41.

[41] Material Safety Data Sheet. (1,3-Dioxolan-2-ylmethyl) triphenylphosphonium bromide[EB/OL]. http://datasheets.scbt.com/sc-222985.pdf

[42] Tavakoli H, Shahrabi T, Hosseini M G. Synergistic effect on corrosion inhibition of copper by sodium dodecylbenzenesulphonate (SDBS) and 2-mercaptobenzoxazole citric acid as an alternative lixiviant for zinc oxide dissolution[J]. Materials Chemistry and Physics,2008, 109(2/3): 281-286.

[43] Abdel-Gaber A M, Abd-El-Nabey B A, Sidahmed I M, et al. Kinetics and thermodynamics of aluminium dissolution in 1.0 mol·L^{-1} sulphuric acid containing chloride ions[J]. Materials Chemistry and Physics, 2006, 98(2/3): 291-297.

[44] Benabdellah M, Touzani R, Dafali A, et al. Ruthenium-ligand complex, an efficient inhibitor of steel corrosion in H_3PO_4 media[J]. Materials Letters, 2007, 61(4/5): 1197-1204.

[45] Ghanbari A, Attar M M, Mahdavian M. Corrosion inhibition performance of three imidazole derivatives on mild steel in 1 mol·L^{-1} phosphoric acid[J]. Materials Chemistry and Physics, 2010, 124(2/3): 1205-1209.

[46] Tuken T, Demir F, Kicir N, et al. Inhibition effect of 1-ethyl-3methylimidazolium dicyanamide against steel corrosion[J]. Corrosion Science, 2012, 59(1): 110-118.

[47] Langmuir I. The constitution and fundamental properties of solids and liquids[J]. Journal of the American Chemical Society, 1916, 38(11): 2221-2295.

[48] Florry P J. Thermodynamics of high polymer solutions[J]. Journal of Chemical Physics, 1942, 10(1): 51-61.

[49] El-Awady A A, Abd-El-Nabey B A, Aziz S G. Kinetic-thermodynamic and adsorption isotherms analyses for the inhibition of the acid corrosion of steel by cyclic and open-chain amines[J]. Journal of Electrochemical Society, 1992, 139(8): 2149-2154.

[50] Lyberatos G, Kobotiatis L. Inhibition of aluminum 7075 alloy corrosion by the concerted action of nitrate and oxalate salts[J]. Corrosion Science, 1991, 47(11): 820-824.

[51] Umoren S A. Synergistic influence of gum arabic and iodide ion on the corrosion inhibition of aluminium in alkaline medium[J]. Portugaliae Electrochimica Acta, 2009, 27 (5): 565-577.

[52] Oguzie E E, Unaegbu C, Ogukwe C N, et al. Inhibooition of mild steel corrosion in sulphuric acid using indigo dye

and synergistic halide additives[J]. Materials Chemistry and Physics, 2004, 84(2/3): 363-368.
[53] Fishtik I F, Vataman I I, Spatar F A. The mechanism of ion-pair formation in the inner part of the double layer[J]. Journal of Electroanalytical Chemistry and Interfacial Electrochemistry, 1984, 165(1/2): 1-8.

柠檬酸中锌防蚀剂(1,3-Dioxolan-2-ylmethyl)三苯基溴化磷和碘离子的协同效应研究

M. Saadawy*
(埃及亚历山大大学理学院化学系, 亚历山大 21321)

摘要：采用称重法、动电位极化法和电化学交流阻抗技术研究了 30 ℃ 时(1,3-Dioxolan-2-ylmethyl)三苯基溴化磷(DTPB)对 0.5 mol·L^{-1} 柠檬酸中锌腐蚀行为的影响. 通过在环保型电解槽中对锌进行酸洗,这在文献中是不常用的. 结果表明,DTPB 作为一种有效的防蚀剂,添加浓度仅为 3×10^{-3} mol·L^{-1} 时,锌在柠檬酸溶液中的防蚀效率可达 98.9%. 由于 DTPB 和碘化钾存在协同效应,两者联用时的防蚀效果要比单独使用 DTPB 强,防蚀参数为 1.2,并随温度升高而减小. 本文提出了碘化钾作为吸附媒介,可使金属表面与 DTPB 结合的防蚀机制.

关键词：锌；极化；电化学交流阻抗；酸蚀；协同